Journal of Genetic Engineering and Biotechnology 23 (2025) 100486

Contents lists available at ScienceDirect

Journal of Genetic Engineering and Biotechnology

journal homepage: www.elsevier.com/locate/jgeb

Whole genome analysis of endophytic strain PM1 reveals promising plant Growth-Promoting mechanisms in pomegranate

Poonam Patel, Fenil Patel *, Chaitanya Joshi, Madhvi Joshi *

Gujarat Biotechnology Research Centre, Gandhinagar, Gujarat 382010, India

ARTICLE INFO

Keywords:
Endophyte
Brucella anthropi
Pomegranate
Plant growth promoting traits (PGPTs)
Secondary metabolites

ABSTRACT

The plant ecosystem harbours diverse symbiotic microorganisms with plant growth promoting and biocontrol activities. The gram- negative endophytic bacterium PM1 strain, isolated from the nodal region of pomegranate. The strain PM1 was studied through whole-genome sequencing, functional annotation, and plant growth-promoting trait (PGPT) gene analysis. Phylogenetic tree analysis and 16S rDNA sequencing confirmed its classification within the genus *Brucella*. The assembled genome size was 5,200,895 bp with a G + C content of 56.4 %. The average nucleotide identity (ANI) analysis revealed a 97.62 % similarity between PM1 and *B. anthropi* ATCC 49188 T, a type strain derived from human clinical samples, indicating a close relationship with *Brucella anthropi.* The functional annotation revealed 2,945 PGPT-related genes, including 32 % linked to direct effects (phytohormone signal production, biofertilization, and bioremediation processes) and 67 % to indirect effects (plant colonization, biocontrol, and competitive exclusion). KEGG analysis revealed genes involved in nitrogen metabolism, phosphate solubilization, siderophore production, hormone biosynthesis (gibberellin, cytokinin, and auxin), root colonization, and stress mitigation. Virulence factor database (VFDB) data revealed the absence of complete virulence gene assemblies, indicating limited pathogenic potential. Furthermore, secondary metabolite analysis predicted the potential production of ochrobactin compounds, which are potent siderophores that are important traits associated with PGPTs. The complete genome analysis of *Brucella* sp. PM1 provides new insights into plant-bacteria interactions, laying a foundation for advanced postgenomic studies and facilitating the development of bioeffective strategies such as biofertilizers or biocontrol agents for sustainable improvement in crop yields.

1. Introduction

Pomegranate (*Punica granatum* L.), which belongs to the *Lythraceae* family, is one of the oldest and most extensively cultivated fruit-bearing crops grown in India.[1–4] The plant provides a wide range of niches for various endophytes including bacterial and fungal endophytes[5]. Bacterial endophytes significantly boost plant growth by inhabiting the intracellular spaces within plant organs. They obtain energy from host-derived amino acids, carbohydrates, and inorganic nutrients[1]. These plant–microbe interactions strengthen plant resilience to both biotic and abiotic stresses.[6–7] The bacterial endophytes contribute to plant growth by inducing the synthesis of phytohormones like Indole-3-Acetic Acid (IAA), which facilitates the dissolution of insoluble phosphates or organic phosphorus compounds, the fixation of nitrogen, synthesis of secondary metabolites, and biocontrol activities through direct or indirect mechanisms. Together, these traits highlight the plant growth-promoting potential (PGPT) of bacterial endophytes.[8–11].

These plant growth promoting (PGP) traits support plant growth and help plants to sustain various stresses within their immediate vicinity, in addition to their own immune and regular metabolic functions. For instance, *Sphingomonas* sp. LK11 found in *Tephrosia apollinea* leaves, which exhibited potential PGPT characteristics such as increased growth and stress tolerance against salt and cadmium.[12] It was also reported that the endophytic genera *Pseudomonas, Arthrobacter*, *Pantoea, Burkholderia*, *Neokomagataea,* and *Psychrobacter* in the roots of *Pennisetum sinese*, were associated with plant growth promotion.[13] From Brassica seeds, *Methylobacterium* sp. was isolated which had capacity to enhance plant growth and act as a biological control agent against the pathogen *Leptosphaeria maculans*.[14].

Despite the importance of pomegranate, only a few studies are available on bacterial endophytes of pomegranate, such as *B. subtilis, S. pyogenes, P. aerogenosa, S. cerevieace*, etc., which exhibit plant growth-

* Corresponding authors.
E-mail addresses: scib6@gbrc.res.in (F. Patel), madhvimicrobio@gmail.com (M. Joshi).

https://doi.org/10.1016/j.jgeb.2025.100486
Received 1 January 2025; Received in revised form 10 March 2025; Accepted 25 March 2025

promoting traits[5,15–16]. Additionally, recent advances in Next generation sequencing (NGS) technologies help to understand microbial genomes in more detail[17]. Whole genome sequencing of endophytic bacteria can unravel the molecular machinery underlying the interactive endophytic life cycle and plant regulatory mechanisms.[18] Despite advancements in NGS technologies, only a single study is available for the complete genome sequence of *Brucella* spp. In this study, the *Brucella anthropi* strain T16R-87 was isolated from the tomato (*Solanum lyco*persicum L.) rhizosphere.[19].

While much is known about traditional PGPR, a substantial gap in understanding of the potential of non-pathogenic *Brucella* species as plant-associated beneficial microbes remains. This study aimed to perform genomic profiling, functional annotation, and assessment of the plant growth-promoting traits of *Brucella* sp. strain PM1 isolated from pomegranate plants. The knowledge of key genes associated with the PGPR potential of *Brucella* sp. strain PM1 could provide new insights into plant–microbe interactions and expand the scope of PGPR research beyond commonly studied genera. The findings of this study may contribute to the development of tailored bioinoculants that improve crop productivity, particularly for economically valuable crops such as pomegranates.

2. Materials and method

2.1. Endophytic bacterial isolation and gram staining

The nodal explants of pomegranate were collected from Dehgam, Gujarat, India (23.1637°N, 72.8102°E). The plant nodal segments were collected and surface sterilized using the following steps: Tween 20 (Himedia, India) treatment for 5 min, fungicide treatment, Bavistin [Carbendazim (50 % WP), Crystal Crop Protection Ltd., India] at 0.1 % for 20 min, antibiotic treatment with Tagmycin (Streptocyclin + Tetracycline 90:10 w/w) (Tropical Agro Pvt. Ltd., India) at 0.1 % for 20 min followed by final wash with $HgCl_2$ (Fisher Scientific, India) at 0.1 % for 5 min and finally rinsed with sterile distilled water (DW) several times. The final wash was spread plated onto nutrient agar as a control. The sterilized explants were inoculated into initiation medium (Muashige and Skoog (MS) (Himedia, India) with 1 mg/L Benzyl Adenine (BA) (Duchefa, The Netherlands) and the cultures were maintained under a day and night cycle of 20/18 °C. During the shooting stage, visible endophytic bacterial growth was observed at the base of nodes.[20] The bacterial cells were cultured on LB (Luria Bertani) agar media (Himedia, India). The bacterial cells were stored in 50 % glycerol stock at −80 °C. For further use, bacteria were cultured on 2 % LB Agar media (Himedia, India) and incubated at room temperature (RT) for 48 h. The colony characteristics were recorded by the standard gram staining method.[20–21].

2.2. 16S rRNA sequencing and phylogenetic identification

For molecular identification of the bacterial isolate, genomic DNA was extracted from an overnight grown culture in LB broth using the QIAamp® DNA Micro Kit (QIAamp Mini, Germany). The concentration and quality of the DNA was assessed using the QIAexpert system (QIAGEN, Germany). The 16S rRNA gene was amplified using the primers 27F (5′ AGAGTTTGATCCTGGCTCAG 3′) and 1429R (5′ GGTTACCTTGTTACGACTT 3′).[22] The PCR system and cycling conditions were performed according to the manufacturer's instructions for the Emerald PCR master mix (Takara Bio Inc., Japan): initial denaturation at 95 °C for 1 min, followed by 30 cycles of denaturation at 95 °C for 1 min, annealing at 58 °C for 50 s, extension at 72 °C for 1.5 min, and a final extension at 72 °C for 7 min. PCR products amplified at 1500 bp were purified using an Exosap IT kit (Thermo Fisher Scientific, USA) and sequenced using an automated DNA sequencer (ABI 3130 XL; Applied Biosystems Instrument, Carlsbad, United States), with BigDye Terminator v 3.1 and a cycle sequencing kit (Thermo Fisher Scientific, USA). The sequencing data were analysed using Codon Code Aligner software (CodonCode Corporation, MA, USA) and culture was identified based on the online BLAST search tool at the National Center for Biotechnology Information (NCBI) Genbank database against non– redundant (NR) database. A phylogenetic tree was constructed using MEGA-X11 software (version 11.0, Mega Limited, Auckland, New Zealand) **(**Tamura et al, 2021**),** which was designed for Molecular Evolutionary Genetic Analysis.

2.3. Biochemical tests for plant growth promoting trait (PGPT)

2.3.1. Indole acetic acid production test

The potential for PGP-related traits was evaluated through various assays. The production of indole acetic acid (IAA) was determined by using the method as described by Marakana et al. (2018) using colorimetric analysis with Salkowski reagent (50 mL, 35 % perchloric acid and 1 mL 0.5 M $FeCl_3$) in the presence of tryptophan. The 1 mL of bacterial supernatant was mixed with 2 mL of salkwoski reagent and incubated for 1 h in the dark. The IAA concentration was determined by measuring absorbance at 450 nm.

2.3.2. Phosphate solubilisation

The potential of the *Brucella* PM1 strain for phosphate solubilisation was qualitatively assessed using Pikovskaya's agar medium (Himedia, Nashik, India). In this method, tricalcium phosphate was used as the phosphorus source, and positive results were indicated by transparent zones around bacterial colonies after a 5 d of incubation period at 30 °C.[23].

2.3.3. Nitrogen fixing ability

The ability to fix nitrogen helps to identify microorganisms that convert atmospheric nitrogen (N_2) into ammonia (NH_3), which can be readily absorbed and utilized by plants. In this method, bacterial growth was checked on Ashby's nitrogen-free medium and incubated at 28 °C for 7 d.[24].

2.3.4. Catalase activity

The catalase activity was determined by the method described by Taylor & Achanzar, (1972). In this method, bubble formation upon the addition of 3 % hydrogen peroxide (H_2O_2) to the bacterial culture confirms a positive reaction.

2.3.5. Siderophore production

The siderophore production of the PM1 strain was determined by the halo zone around colonies of the PM1 strain on Chrome azurol S (CAS) medium incubated at 28 °C for 2–4 d.[25].

2.4. Library preparation and whole genome sequencing

The extracted DNA, which was used for 16S rDNA gene sequencing, was further quantified using the Qubit dsDNA HS Assay Kit with a Qubit fluorometer 4.0 (Thermo Fisher Scientific, USA). The shotgun libraries were prepared following the instructions provided by the manufacturer using the Illumina Nextera XT DNA Library Preparation Kit (Illumina Inc., USA). The quality of the libraries was assessed using the Agilent Bioanalyzer 2100 (Agilent, USA), and their quantification was performed using the Qubit Fluorometer (Thermo Fisher Scientific, USA). The normalized libraries were pooled up to a concentration of 4 nM, denatured, and loaded onto the Illumina MiSeq sequencing platform. The sequencing was carried out using the Illumina MiSeq 500 cycle reagent kit V2.

2.5. Genome assembly and annotation

The quality of the raw sequencing reads was evaluated using FastQC.[26] The low-quality reads were filtered out by using Trimmomatic

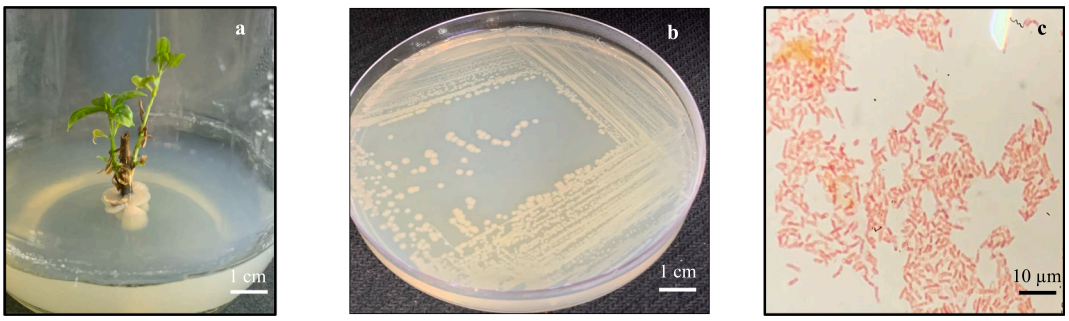

Fig. 1. Representative image of endophytic bacteria strain PM1 isolated from pomegranate nodal region (a), isolation of endophytic bacteria on LB plate (b) and Gram's staining of bacteria (c). Scale – 1 cm (a and b) and 10 µm (c).

with a minimum length of 50 bp and an average quality score of < 20. To assemble the genome, the SPAdes was used[27] and for genome identification, the Type Strain Genome Server (TYGS), was used[28]. The whole genome was annotated using the DDBJ Fast Annotation and Submission Tool (DFAST) version 1.2.15[29] and PATRIC server: Bacterial and Viral Bioinformatics Resource Center (BV-BRC) version 3.28.5.[30] The functional annotations were performed using Omicsbox (https://www.biobam.com), Eggnog-Mapper[31] and KEGG database (KofamKOALA version 104.0).

2.6. Functional annotation of plant growth promoting traits

For predicting PGPTs associated with the bacterial genome, functional annotation was performed using the PLaBase (PLant-associated BActeria web resource) tool version 1.02, (PGPT-Pred subtool).[32] For molecular network reconstructions and assigning KO IDs (KEGG Orthology IDs), the KEGG database (KofamKOALA version 104.0) was used.[33] Furthermore, KEGG Mapper was used for pathway annotations of genes associated with gibberellin, auxin, and cytokinin biosynthesis; nitrogen metabolism and assimilation; nitrification; phosphate solubilisation and transport; root colonisation; and responses to various stresses, including cold, heat shock, oxidative, and heavy metal stress.

2.7. Prediction of virulence factors and secondary metabolite biosynthetic related gene clusters

The genome was also analysed for the presence of any virulent factors using Virulence Factor Database Genome sequences (VFDB).[34] The identification of secondary metabolite biosynthesis gene clusters in the genome was carried out using antiSMASH 6.0.[35].

3. Results

3.1. Morphology and phylogenetic analysis

The morphological observations of the isolated bacteria exhibited white, round-shaped colonies of medium size with moist surface characteristics on LB medium. Additionally, Gram staining indicated a Gram-negative profile (Fig. 1).

A phylogenetic tree was constructed for the isolated endophyte PM1 based on the BLAST results using MEGA-X11. It showed 100 % sequence similarity with the *B. lupini* strain NRBC 102587 on the basis of BLAST results. Additionally, a phylogenetic tree was constructed by using the maximum-likelihood method (Bootstrap method: 1000 replications, Model: Tamura-Nei model) based on the 16S rDNA sequences of 12 species closely related to the *Brucella* genus. The 12 endophytic strains belong to *lupini*,[36] *ciceri* (*Cicer arietinum*),[37] oryzae (*Oryzae sativa* L.), cysiti (*Cytisus scoparius*),[38] grignonensis and tritici (wheat)[39] from plants and *intermedia*, *endophytica, rhizosphaerae and soli* are from other as they produced top hits from NCBI BLAST data. The PM1 was clustered in the same clade as *Brucella tritici* SCII24 and further subclustered with *Brucella lupini* NBRCC 102587 and *Brucella anthropi* ATCC 49188 (Fig. 2). The 16S sequence data has been submitted in NCBI GenBank with accession number PV243290.

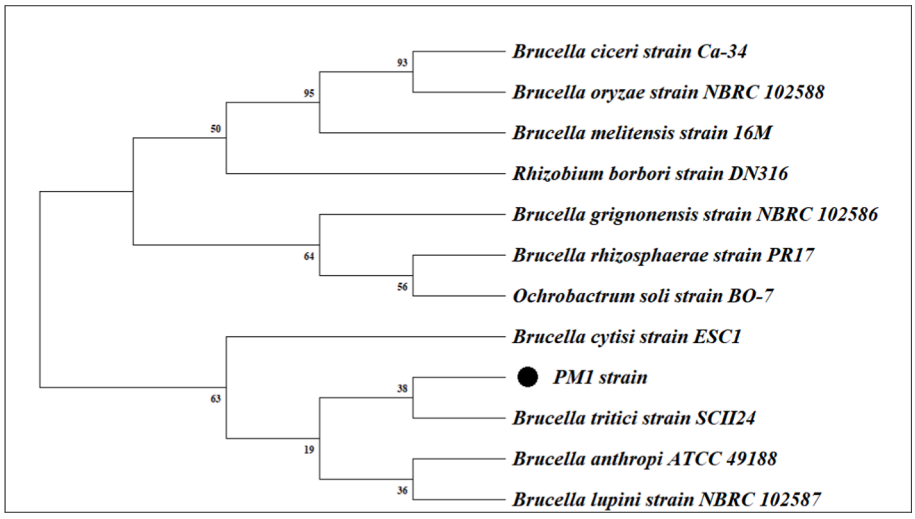

Fig. 2. Phylogenetic tree of PM1 was inferred by using the Maximum Likelihood method and Tamura-Nei model based on 16S rDNA sequences. Branch support was evaluated through bootstrap analysis with 1000 replications, and the resulting bootstrap values are displayed at the respective nodes.

Table 1
Plant growth promoting traits of strain PM1.

Bacterial isolate	Production assay				
	IAA production	Phosphatase activity	Catalase	Nitrogen fixation	Siderophore production
Strain PM1	+ 51.22 ± 0.16 μg mL^{-1}	+	+	+	+

'+' – indicates positive results.

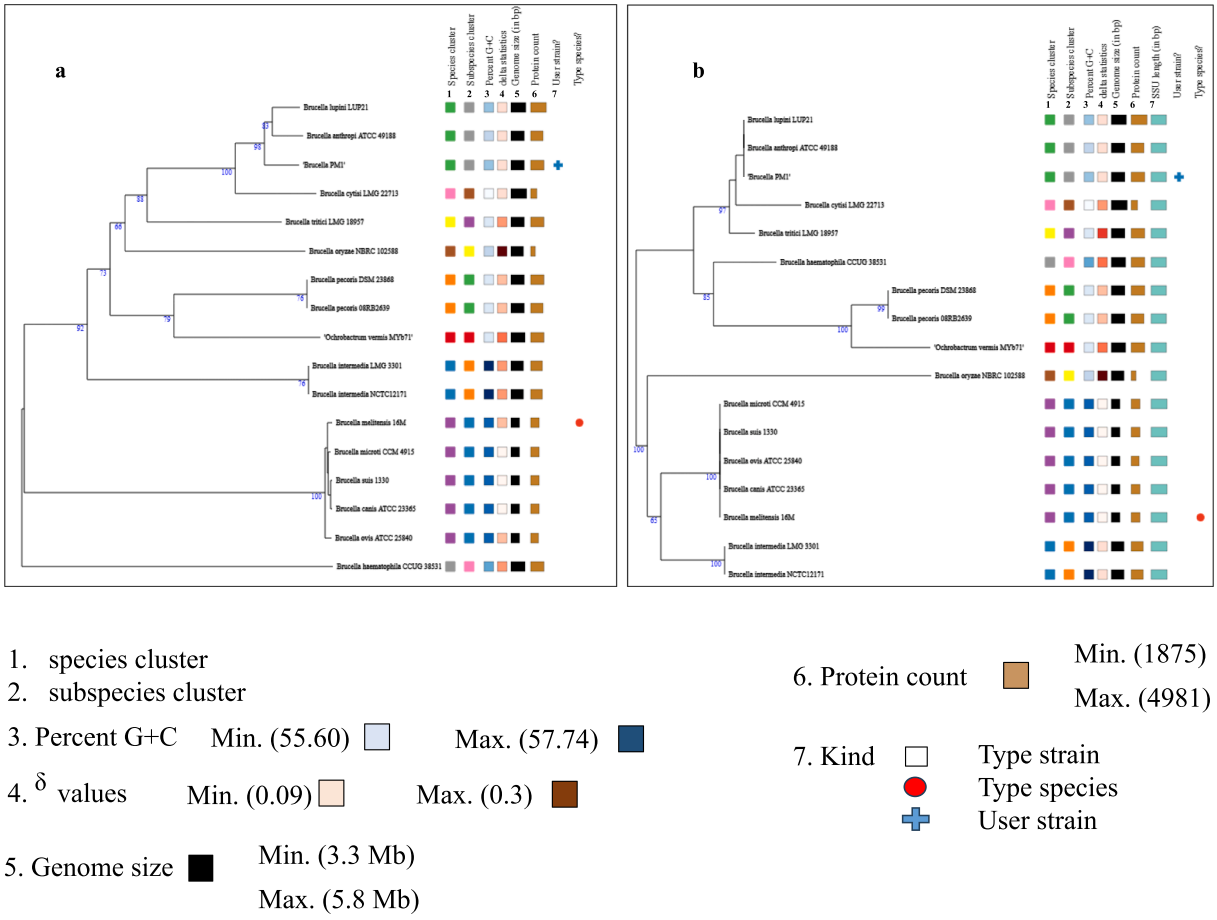

Fig. 3. Genome based taxonomy of Brucella strain PM1 using Type strain genome server results whole genome based (a) and 16S rDNA based (b). Tree was predicted with FastME 2.1.456 from GBDP distances calculated from genome sequences. Branch lengths are scaled in terms of GBDP distance formula d5; numbers above branches are GBDP pseudo-bootstrap support values from 100 replications. Leaf labels are annotated by affiliation to species (1) and subspecies (2) clusters, genomic G + C content (3), δ values (4), overall genome sequence length (5), number of proteins (6), and the kind of strain (7). User-provided GenBank accession IDs are shown in parentheses; master record accessions are truncated.

3.2. Plant-growth promoting traits of the strain PM1

The result showed a potential production of 51.22 ± 0.16 μg/mL IAA (plant-growth-promoting hormone) from strain PM1 in the presence of tryptophan (1 mg/mL). The qualitative assays represented the ability of the PM1 strain to solubilise inorganic phosphate with a halo zone around a colony grown on a Pikovskaya agar plate. The nitrogen fixation ability was confirmed by the growth of the PM1 strain over Ashby's medium. Bubble formation in the presence of 3 % H_2O_2 was positive, indicating the potential of antioxidant defence mechanisms. Further, the production of halo zones on CAS agar plates confirmed the production of siderophore (Table 1).

Table 2
Genome features and assembly Statistics of *Brucella anthropi* strain PM1.

Features	DFAst	BV-BRC
Total Length	5,200,895 bp	5,200,895 bp
N50	259,897	259,897
L50	–	6
GC Content (%)	56.4	56.31
CDS	5,106	5,402
tRNA	51	48
rRNA	3	3
CRISPR elements	0	0

3.3. Genome based taxonomy and assembly statistics

After the trimming of whole genome sequencing data, a total of 487,187 high-quality paired-reads were obtained, which corresponds to approximately 324 Mb of data. This represented 55X genome coverage overall. The SPAdes assembler generated a total of 48 contigs, with an N50 value of 20,4814 bp. The TYGS data confirmed the identification of the genome as *B. anthrxopi* based on the basis of the whole genome and 16S rDNA of the available genome (Fig. 3). The average nucleotide

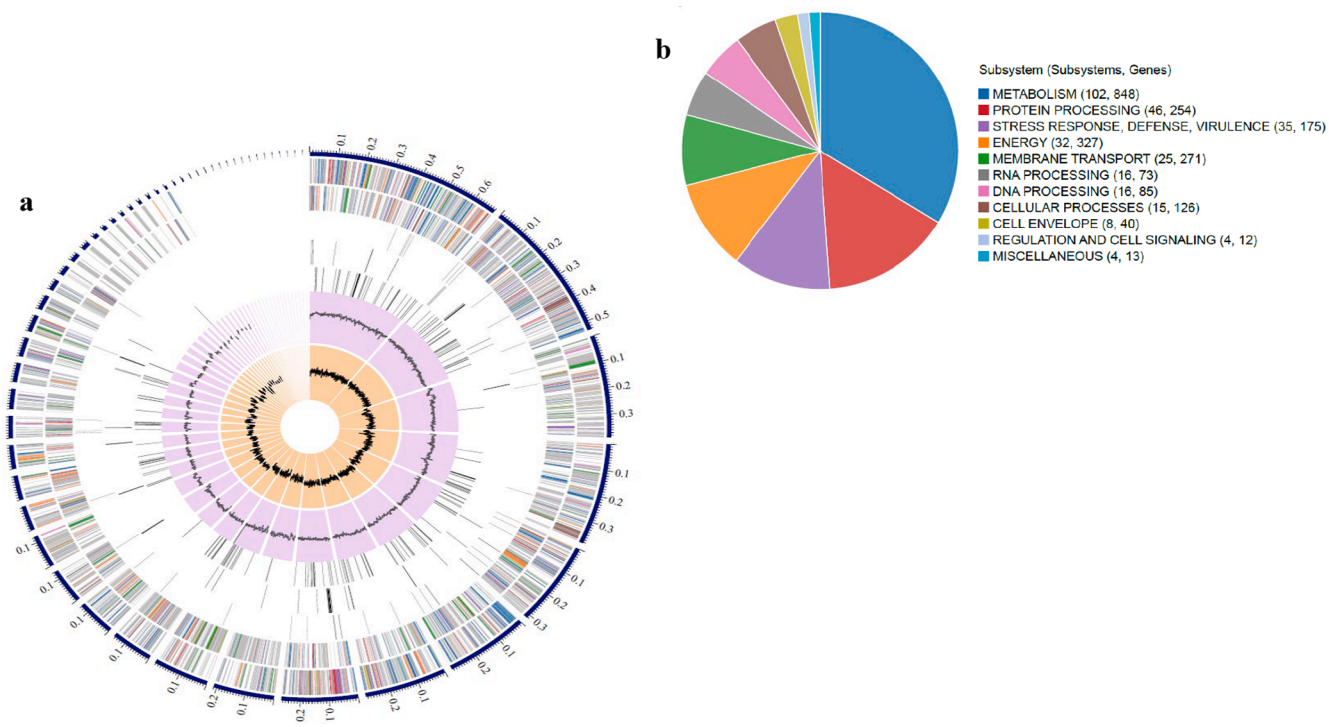

Fig. 4. A circular representation of the *B. anthropi* PM1 genome (5,200,895 bp). This includes, from outer to inner rings, the contigs, CDS on the forward strand, CDS on the reverse strand, RNA genes, CDS with homology to known antimicrobial resistance genes, CDS with homology to know virulence factors, GC content and GC skew (a). The colors of the CDS on the forward and reverse strand indicate the subsystem that these genes belong to. A subsystem is a set of proteins that together implement a specific biological process or structural complex and annotation includes an analysis of the subsystems unique to each genome (b).

identity (ANI) resolves strains of the same or closely related species with values ranging between 80 % and 100 %.[40] In the present study, ANI analysis performed by DFAST tool yielded a conclusive match of 97.62 % with strain PM1. Additionally, genome sequence assembly statistics obtained from DFAST revealed a sequence length of 5,200,895 bp, an N50 value of 259,897 bp, a G + C content of 56.4 %, and a coding ratio of approximately 86.3 %. The PM1 strain contains 51 tRNAs and 3 rRNAs for noncoding RNA. Furthermore, the BV-BRC tool analysis confirmed the genome characteristics, reporting a total genome length of 5,202,017 bp, an N50 value of 5,200,895, an L50 value of 6, and a G + C content of 56.37 % (Table 2, Fig. 4). The genomic data has been submitted to NCBI GenBank with accession number SAMN47257544 under bio project number PRJNA1233178.

3.4. Functional genome annotation

The functional annotation of the PM1 genome was performed by a BLAST search, in which the putative protein-coding sequences were used to query against the COG (EggNOG mapper), interproscan (Omicsbox), and KEGG (Kofamkoala) databases (Fig. 5). Most of the predicted genes (83.57 %) could be assigned to one of 25 functional clusters of orthologous groups (COGs), and 16 % were classified as proteins of unknown function, while the remaining genes were annotated as hypothetical proteins. The distribution of genes into COG functional categories is presented in Table 3 (Fig. 5a). Further, the interproscan data showed 2245 (61.2 %) annotated genes for the 3 main GO categories of biological process, cellular component, and molecular function with 48 categories using omics box analysis. The molecular function component was distributed across ATP binding activity, ion binding, and transferase activity (Fig. 5b (i)). The biological process consists of the regulation of the DNA template, transmembrane transport, DNA integration, and cellular processes (Fig. 5b (ii and iii)). The functional distribution of strain PM1 was further annotated using the KEGG database, which assigned 2,758 (53.4 %) genes to 45 different KEGG pathways to gain deeper insights into its functions. Gene functions were categorized into five main groups: Cellular Process, Environmental Information Processing, Genetic Information Processing, Metabolism, and Organismal Systems. Each of these categories was further subdivided into specific subcategories with the allocated genes (Fig. 5c).

3.5. Identification of plant growth-promoting traits associated with b. Anthropi PM1

To understand the PGPTsof the *B. anthropi* strain PM1 in connection with the *Lythraceae* family, a functional analysis of the annotated genome was conducted. This analysis aimed to identify various PGPT indicators, such as indole-3-acetic acid (IAA) production, gibberellin biosynthesis, nitrogen fixation, phosphate solubilisation, siderophore production, and other related genes. These indicators serve as valuable predictors of plant growth.[37] For this study, the PLaBAse database (specifically the PGPT viewer) was utilised to identify genes, proteins, and pathways associated with PGPTs in *B. anthropi*. A total of 2,945 genes were allocated as potential PGPTs across the *B. anthropi* genome. These genes were predominantly associated with indirect effects (68 %), including plant colonization, biocontrol, and competitive exclusion. The remaining 32 % represented genes associated with direct effects such as biofertilisation, phytohormone signal production, and bioremediation processes (Fig. 6). The direct effects related to bio-fertilization involved primarily phosphate and potassium solubilisation, iron and nitrogen acquisition, sulphur assimilation, and CO_2 acquisition (Fig. S1 (a)). These processes directly promote nutrient availability and support plant growth. The category of phytohormone signal production encompassed genes associated with the production of vitamins, signalling volatile compounds, embryogenesis, germination stimulation signals, and auxin and cytokinin metabolism (Fig. S1 (b)). The bioremediation class included genes associated with heavy metal detoxification (mainly iron, nickel, copper, and cobalt) and the degradation of xenobiotic such as hydrocarbons, aromatic hydrocarbons, benzoate, styrene, organophosphates, and naphthalene (Fig. S1 (c)).

3.6. Genes associated with plant growth promoting (PGP) traits

The PGP traits related to the PM1 strain were confirmed *in vitro via* IAA production, phosphate solubilisation, nitrogen fixation, catalase activity and siderophore production. Further, the genes associated with plant growth-promoting traits were screened across various metabolic pathways in relation to plants to gain a deeper understanding of the underlying mechanism.

The gene clusters associated with IAA (Auxin) production were identified in the PM1 genome. Tryptophan is a precursor of IAA synthesis in bacteria. In this study, a set of kynurenine pathways was identified for tryptophan metabolism (Fig. S2 (a)), and the tryptophan biosynthesis gene set *trpA, trpc, trpD, PIN, PILS, and ECM3* were also observed in the KEGG pathway map (Fig. S2(b), Table 4). The other gene sets corresponding to gibberellin biosynthesis including *GID1, CYP, GA2ox, GA20ox, GA3ox* and *GA13ox* (Fig. S3 (a)) and those related to cytokinin biosynthesis such as *LOG, CKX, AHK2_3_4, IPT, miaA, TRIT1, NDPS1* and miaB (Fig. S3 (b)) were also identified in the PM1 genome (Table 4). Further, genes associated with the phosphate metabolism pathway, including the phosphate transporter encoding genes *pstS, pstC, pstA, pstB* and *phoB* were annotated (Table 5, Fig. S4). The data were further validated through biochemical tests, with halo zones observed around PM1 on Pikovskaya agar plates, indicating solubilisation of inorganic phosphate.

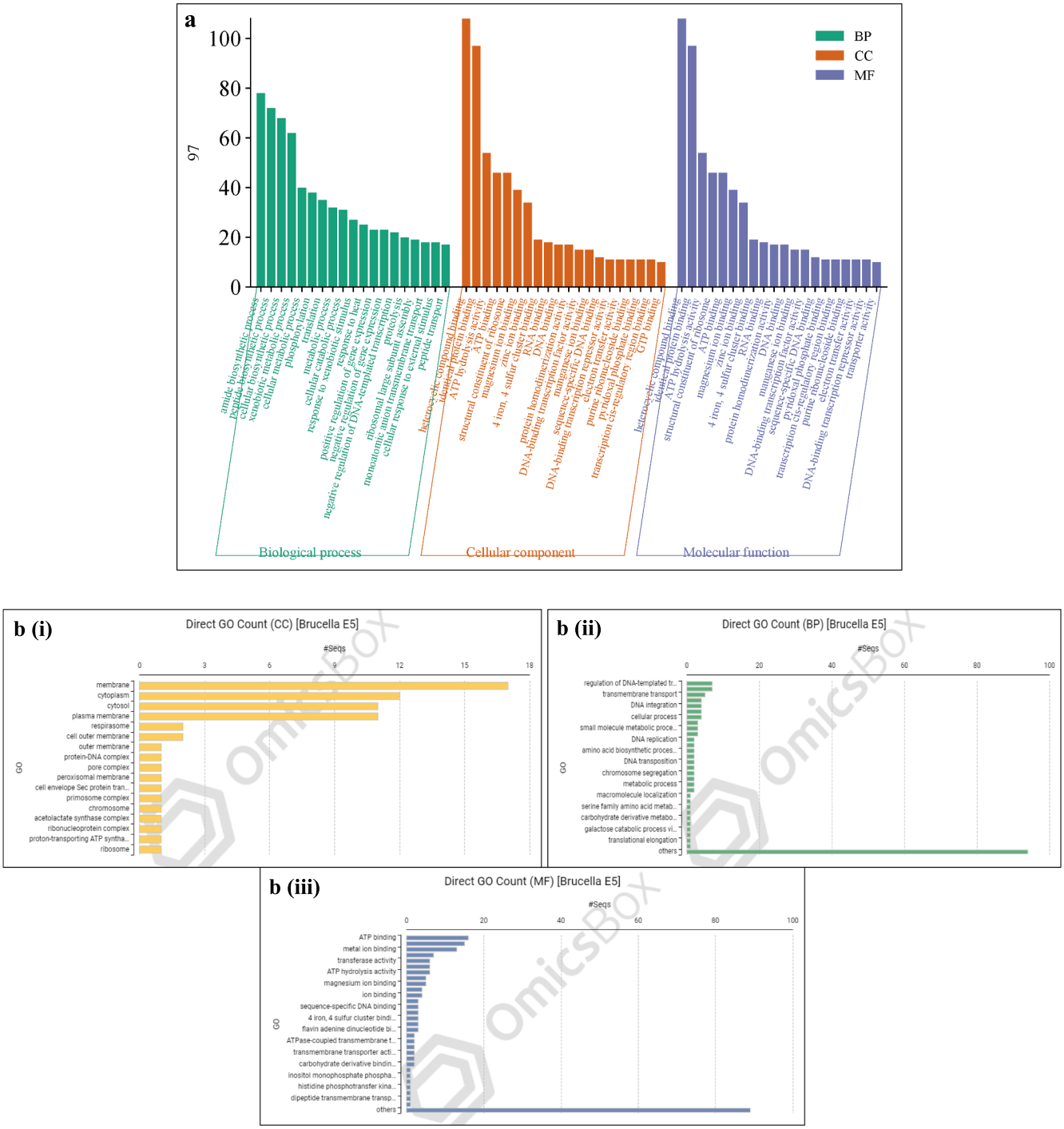

Fig. 5. The genome annotation information of the predicted gene functions of PM1 strain based on COG (a) and Interproscan (b) and KEGG (c) databases.

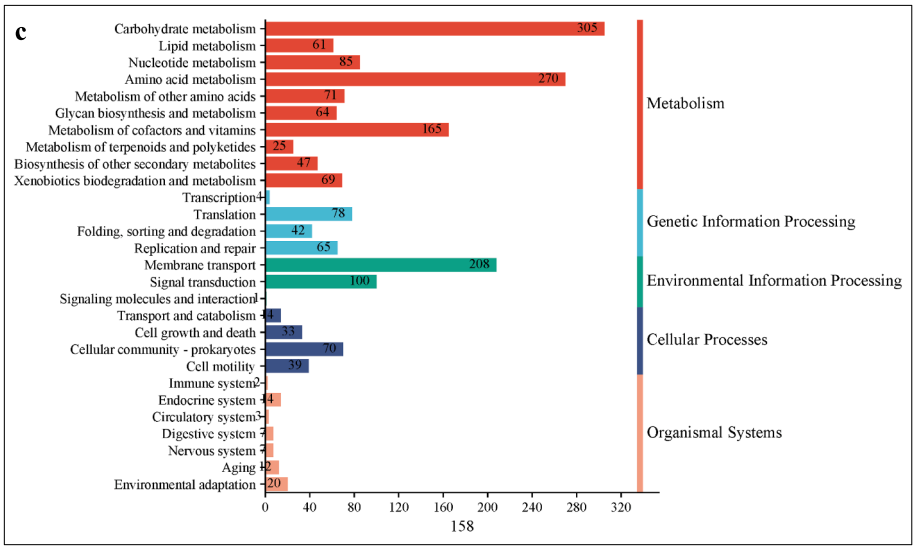

Fig. 5. (*continued*).

Table 3
Number of genes associated with general COG functional categories.

Category	Genes	%	Description
A	0	0.0	RNA processing and modification
B	1	0.0	Chromatin structure and dynamics
C	12	0.6	Energy production and conversion
D	31	1.5	Cell cycle control, cell division, chromosome part
E	252	12.0	Amino acid transport and metabolism
F	152	7.2	Nucleotide transport and metabolism
G	120	5.7	Carbohydrate transport and metabolism
H	34	1.6	Coenzyme transport and metabolism
I	86	4.1	Lipid transport and metabolism
J	0	0.0	Translation, ribosomal structure, and biogenesis
K	128	6.1	Transcription
L	69	3.3	Replication, recombination, and repair
M	123	5.9	Cell wall/membrane/envelope biogenesis
N	34	1.6	Cell motility
O	87	4.1	Posttranslational modification, protein turnover, chaperones
P	218	10.4	Inorganic ion transport and metabolism
Q	47	2.2	Secondary metabolites biosynthesis, transport, and catabolism
S	286	13.6	General function prediction only
T	337	16.0	Functions unknown
U	59	2.8	Signal transduction mechanisms
V	29	1.4	intracellular trafficking, secretion, and vesicular
W	0	0.0	Defense mechanisms
X	0	0.0	Extracellular structures
Y	0	0.0	Nuclear structure
Z	0	0.0	Cytoskeleton
–	4	0.2	Not in EggNOG

Gene clusters associated with biological nitrogen fixation were identified viz. *nirK, narG, narZ, nxrA, narH, narY, nxrB, narI, narV, nosZ, norC and norB* along with key regulatory genes involved in nitrogen metabolism such as *gltB glnA, GLUL, gltD, nirK, arc, narG, narZ, nxrA, narH, narY, nxrB, narI, narV, NosZ, ncd2, npd, cynT, can, NRT2, narK, nrtP* and *nasA* (Table 5, Fig. S5). These findings were reconfirmed by the growth of PM1 in nitrogen-free media. Additionally, gene clusters related to potent siderophore activity and root colonisation were also annotated, depicting their roles in nutrient availability and plant interaction (Table 5).

Further, gene clusters with potential roles in combating abiotic stresses were also annotated. These include genes encoding cold-active chaperones (*cspA*), Heat shock proteins (*hslR, hspQ, htpX, hslJ*), oxidative stress (*SOD2, SOD1*, *trxB*, TRR, *trxA, dsbD, dipZ, ybbN*) and heavy metal stress proteins (*atm1, pexA*, *ABC.PE.S*, *czcD, zitB*) (Table 6).

3.7. Annotation of virulence factors

The comparison of the annotated genomes of *B. anthropi* and plant bacteria only interaction factor (PIFAR) proteins was carried out. The results showed that the isolated bacterium has the ability to interact with plants. However, the identified factors were also associated with pathogenicity. The analysis revealed the following distribution of factors: 23 % virulence factors (such as syringomycin and toxoflavin), 19 % exopolysaccharides (EPSs) (including amylovoran and gumH), 16 % hormone-related factors (such as salicylic hydroxylase, IAA, and cytokinin), 12 % detoxification factors (including isothiocyanate), 9 % factors related to metabolism and adhesion, 6 % multidrug resistance factors, and 5 % factors related to lipopolysaccharide (LPS) and protease activity (Fig. S6).

For further analysis, the Virulence Factor Database(VFDB) was used. The results showed that out of a total of 4261 putative identified genes, 2931 sequences were aligned with Brucella PM1. Notably, four proteins of isolate PM1 were found to be linked with known virulence proteins from other pathogens in a range of 25 % – 30 % similarity. The significantly aligned virulence proteins were as follows: the transcriptional regulator PtxR (ptxR) (a nutritional/metabolic factor), the DNA-binding transcriptional activator AllS (related to allantoin utilisation-a nutritional/metabolic factor), transcriptional regulator (related to pyoverdine-a nutritional/metabolic factor) (PA2383), and LysR family transcriptional regulator (related to HemO cluster – a nutritional/metabolic factor) (Table 7).

3.8. Secondary metabolite production

The antiSMASH tool was used to find out secondary metabolite production. It produced 9 gene clusters with 4 % – 85 % similarity with previously reported gene clusters of secondary metabolite production (Table 8). The gene clusters included amabactin, oryzanaphthopyran A, oryzanaphthopyran B, oryzanaphthopyran C, oryzanthrone A, oryzanthrone B, chlororyzanthrone A, chlororyzanthrone B, Corynecin III/ Corynecin II/ Corynecin I and Orchrobactin (Fig. 7 (a, b), Table 8).

4. Discussion

Bacterial endophytes colonise various plant compartments by dispersing from the soil and rhizosphere, forming mutual associations with the host.[41] Bacterial endophytes *in vivo* exhibit various plant growth promoting and biocontrol traits. Their plant growth promoting

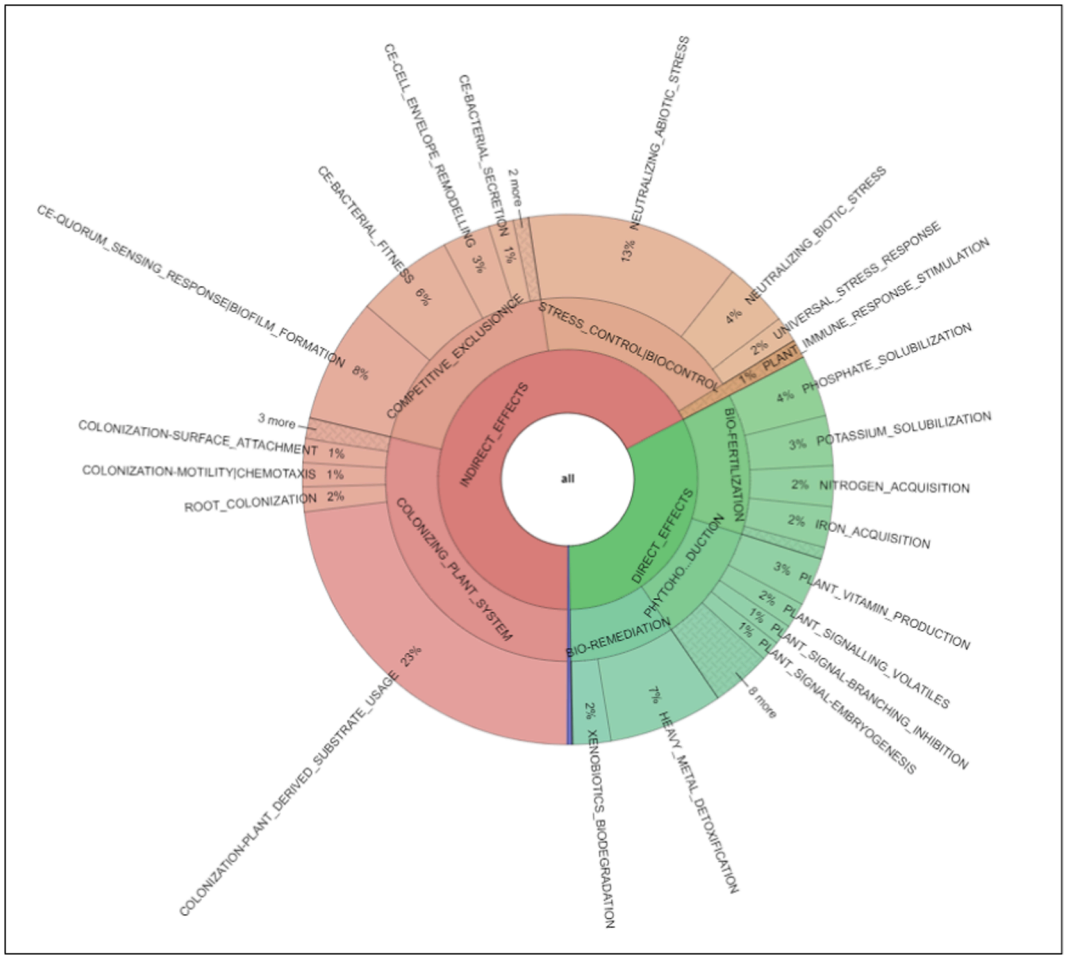

Fig. 6. The Krona plot depicting the predicted PGPT (plant-Brucella interaction) from the PGPT tool (PLabase). BlastP and HMMER annotation against the PGPT-BASE were used to identify PGPT. Level three of six annotation depth is presented here.

Table 4
Genes corresponding plant growth promoting through various phytohormones signalling metabolic pathways in *Brucella* genome.

Metabolic pathway	Genes	Product	KO ID	Locus
Auxin (IAA)	*trpD*	anthranilate phosphoribosyltransferase	K00766	fig|1201037.14.peg.2200
biosynthetic pathways	*trpC*	indole-3-glycerol phosphate synthase	K01609	fig|1201037.14.peg.2199
	trpA	tryptophan synthase alpha chain	K01695	fig|1201037.14.peg.4056
	trpEG	anthranilate synthase	K13503	fig|1201037.14.peg.1741
	trpB	tryptophan synthase beta chain	K01696	fig|1201037.14.peg.4054
	PIN	auxin efflux carrier family protein	K13947	fig|1201037.14.peg.1887
	PILS, ECM3	auxin efflux carrier family protein	K24139	fig|1201037.14.peg.1887
Cytokinin biosyntheis pathways	*LOG*	cytokinin riboside 5′-monophosphate phosphoribohydrolase	K22522	fig|1201037.14.peg.1576
	CKX	cytokinin dehydrogenase	K00279	fig|1201037.14.peg.1932
	AHK2_3_4	arabidopsis histidine kinase 2/3/4 (cytokinin receptor)	K14489	fig|1201037.14.peg.1712
	IPT	adenylate dimethylallyltransferase (cytokinin synthase)	K10760	fig|1201037.14.peg.1952
	miaA, TRIT1	tRNA dimethylallyltransferase	K00791	fig|1201037.14.peg.1952
	NDPS1	dimethylallylcistransferase	K18114	fig|1201037.14.peg.2184
	miaB	tRNA-2-methylthio-N6-dimethylallyladenosine synthase	K06168	fig|1201037.14.peg.3998
Gibberellin biosynthesis	*GID1*	gibberellin receptor GID1	K14493	fig|1201037.14.peg.3733
	CYP714B	gibberellin 13-oxidase	K20666	fig|1201037.14.peg.5018
	CYP714A2	gibberellin 13-/12alpha-oxidase	K20662	fig|1201037.14.peg.5018
	CYP714D1	gibberellin 16alpha,17-epoxidase	K20663	fig|1201037.14.peg.5018
	GA2ox	gibberellin 2beta-dioxygenase	K04125	fig|1201037.14.peg.88
	GA20ox	gibberellin-44 dioxygenase	K05282	fig|1201037.14.peg.88
	GA3ox	gibberellin 3beta-dioxygenase	K04124	fig|1201037.14.peg.88
	GA13ox	gibberellin 13-oxidase	K24460	fig|1201037.14.peg.88

activities include nitrogen fixation and the production of various phytohormones, while biocontrol strategies involve nutrient competition, mineral availability and siderophore production.[42].

The 16S rDNA sequencing analysis identified the bacterium PM1 as *Brucella lupini*.[43] However, the 16S rRNA gene serves as a conserved marker for bacterial classification, and genome-based phylogenetic analysis offers greater reliability.[44] Hence, the sequenced genome (5,200,895 bp) of Brucella strain PM1 closely aligns with those reported

Table 5
Genes corresponding plant growth promotion through various plant colonizing metabolic pathways in *Brucella* genome.

Metabolic pathway	Genes	Product	KO ID	Locus tag
	arcC	carbamate kinase	K00926	fig|1201037.14.peg.4429
	narG, narZ, nxrA	nitrate reductase / nitrite oxidoreductase, alpha subunit	K00370	fig|1201037.14.peg.3720
	narH, narY, nxrB	nitrate reductase / nitrite oxidoreductase, beta subunit	K00371	fig|1201037.14.peg.3719
	narI, narV	nitrate reductase gamma subunit	K00374	fig|1201037.14.peg.3717
	NosZ	nitrous-oxide reductase	K00376	fig|1201037.14.peg.4317
	ncd2, npd	nitronate monooxygenase	K00459	fig|1201037.14.peg.1143
	cynT, can	carbonic anhydrase	K01673	fig|1201037.14.peg.3758, fig|1201037.14.peg.2980
	NRT2, narK, nrtP, nasA	nitrate/nitrite transporter	K02575	fig|1201037.14.peg.3721
Phosphate transport	*PstS*	phosphate transport system substrate-binding protein	K02040	fig|1201037.14.peg.4013
	pstC	phosphate transport system permease protein	K02037	fig|1201037.14.peg.4012
	pstA	phosphate transport system permease protein	K02038	fig|1201037.14.peg.4011
	pstB	phosphate transport system ATP-binding protein	K02036	fig|1201037.14.peg.4010
	phoB	phosphate regulon response regulator PhoB	K07657	
Iron transport	*feoB*	ferrous iron transport protein B	K04759	fig|1201037.14.peg.1536
	feoC	ferrous iron transport protein C	K07490	fig|1201037.14.peg.1695
	FTR, FTH1, efeU	high-affinity iron transporter	K07243	fig|1201037.14.peg.1602
	ABC.MN.P	manganese/iron transport system permease protein	K09819	fig|1201037.14.peg.1518
	SMF	metal iron transporter	K12346	fig|1201037.14.peg.1899
siderophore transport	*fagD, cchF, irp1A, piaA*	iron-siderophore transport system substrate-binding protein	K25286	fig|1201037.14.peg.3792
	fepD, fagA, cchC, desH	iron-siderophore transport system permease protein	K23186	fig|1201037.14.peg.3793
	fepG, fagB, cchD, desG	iron-siderophore transport system permease protein	K23187	fig|1201037.14.peg.3794
	fepC, fagC, cchE, desF	iron-siderophore transport system ATP-binding protein	K23188	fig|1201037.14.peg.3795
	yclP, ceuD	iron-siderophore transport system ATP-binding protein	K25285	fig|1201037.14.peg.76
	yclO, ceuC	iron-siderophore transport system permease protein	K25283	fig|1201037.14.peg.77
	yclN, ceuB	iron-siderophore transport system permease protein	K25284	fig|1201037.14.peg.78
	fepC, fagC, cchE, desF	iron-siderophore transport system ATP-binding protein	K23188	fig|1201037.14.peg.1101
Root colonization	*mcp*	methyl-accepting chemotaxis protein	K03406	fig|1201037.14.peg.734
	motA	chemotaxis protein MotA	K02556	fig|1201037.14.peg.1275
	motB	chemotaxis protein MotB	K02557	fig|1201037.14.peg.1293
	motC	chemotaxis protein MotC	K10564	fig|1201037.14.peg.1294
	motD	chemotaxis protein MotD	K10565	fig|1201037.14.peg.1295
	hss	homospermidine synthase	K00808	fig|1201037.14.peg.1226
	aer	aerotaxis receptor	K03776	fig|1201037.14.peg.734

for *B. anthropi* strain ATCC 49188 in the NCBI database. Additionally, the data fell within the expected range of quality and aligned with other strains, confirming the accuracy and reliability of the genome assembly results. For further analysis, 16S rRNA gene sequences of a total of 12 closely related species belonging to the *Brucella* genus were obtained, and a phylogenetic tree was constructed to validate the classification of the PM1 bacterium.

The *Brucella* and plant interaction involves the annotation of allied genes encoding positive PGPTs. In the present study, a total of 2,945 PGPTs, representing both direct (32 %) and indirect (68 %) effects of *Brucella* sp. PM1 on plant growth were identified. Similar studies have shown the effects of *Brucella* on *Leclercia tamurae* sp. nov. and *Silvania gen.* nov. isolated from the oak rhizosphere with 5,500 and 5,638 PGPTs, respectively, categorised into direct (28 %) and indirect (72 %) effects.[45] Imran et al., (2014) also reported that *Ochrobactrum* sp. Pv2Z2 increased plant growth through enhanced nutrient uptake and solubilisation. Meng et al., (2014) found that *O. anthropi* Mn1 promoted nitrogen fixation and IAA production, leading to root formation. These findings highlight the potential of *Brucella* sp. and related bacteria as beneficial microorganisms for enhancing plant growth based on available genomic information.

In the present study, genes of the PM1 strain that are associated with plant growth-promoting phytohormones such as auxin, cytokinin, and gibberellin were identified. This finding aligns with similar studies on endophytes such as *Sphingomonas* sp. LK11[12] and *Pseudomonas aeruginosa* B-18 (Dos Santos HRM et al., 2019), which also showed the presence of genes involved in indole-3-acetic acid (IAA) production. Other studies on *Sphingomonas* sp. LK11 demonstrated the presence of genes related to gibberellin biosynthesis.[12] Additionally, strains of *Bacillus* sp.[47] and *Methlyobacterium* sp.[48] were found to possess genes responsible for cytokinin production. These results emphasise the prevalent presence of genes linked to phytohormone synthesis in diverse endophytic bacteria, encompassing *B. anthropi* strain PM1.

The PGP traits of the PM1 strain were confirmed *in vitro via* IAA production, phosphate solubilisation, nitrogen fixation, catalase activity, and siderophore production. Further, the genes associated with plant growth promotion traits were screened across various metabolic pathways with plants to gain a deeper understanding of the underlying mechanism. The gene clusters associated with IAA (auxin) production, gibberellin biosynthesis, and cytokinin biosynthesis were identified in the PM1 genome in the present study. Further, genes linked to the phosphate metabolism pathway, including the phosphate transporter-encoding genes *pstS, pstC, pstA, pstB* and *phoB*, were annotated (Table 5, Fig. S4). The data were further validated through biochemical tests, with observed halo zones around the PM1 on Pikovskaya agar plates, indicating solubilisation of inorganic phosphate. The other researchers have also identified similar gene sets in *Bacillus halotolerans* Q2H2 (*trpABCDE*),[49] *Sphingomonas* LK11 (*trpABD*)[50] and *Enterobacter cloacae* UW5.[51].

Gibberellins are essential phytohormones in plants that regulate seed germination, stem elongation, and flowering processes.[52] The PM1 genome has many genes related to gibberellins (Table 4), which are responsible for the biosynthesis of a key gibberellin compound, GA4. Bacterial gibberellin biosynthesis typically involves cytochrome P450 (CYP)-rich operons, as observed in *Bradyrhizobium japonicum* (*CYP112, CYP114*, and *CYP117*)[53]. Interestingly, a recent report suggests that GA3

Table 6
Genes encoding stress responsiveness in *Brucella* genome.

Stress related Proteins	Genes	Product	KO ID	Locus tag
Cold active chaperones	*cspA*	cold shock protein	K03704	fig|1201037.14.peg.1800
Heat shock proteins	*hslR*	ribosome-associated heat shock protein Hsp15	K04762	fig|1201037.14.peg.1447
	hspQ	heat shock protein HspQ	K11940	fig|1201037.14.peg.1372
	htpX	heat shock protein HtpX	K03799	fig|1201037.14.peg.1494
	hslJ	heat shock protein HslJ	K03668	fig|1201037.14.peg.2694
Oxidative stress	*SOD2*	superoxide dismutase, Fe-Mn family	K04564	fig|1201037.14.peg.4698,
	SOD1	superoxide dismutase, Cu-Zn family	K04565	fig|1201037.14.peg.46
	trxB, TRR	thioredoxin reductase	K00384	fig|1201037.14.peg.1816
	trxA	thioredoxin 1	K03671	fig|1201037.14.peg.4059
	dsbD, dipZ	thioredoxin:protein disulfide reductase	K04084	fig|1201037.14.peg.4658
	ybbN	putative thioredoxin	K05838	fig|1201037.14.peg.432
Heavy metal stress	*atm1, pexA*	ATP-binding cassette, subfamily B, heavy metal transporter	K24821	fig|1201037.14.peg.361
	ABC.PE.S	peptide/nickel transport system substrate-binding protein	K02035	fig|1201037.14.peg.1515
	czcD, zitB	cobalt-zinc-cadmium efflux system protein	K16264	fig|1201037.14.peg.567

Table 7
Significant virulence proteins identified using virulence factor database (VFDB).

Sr. no.	Virulence proteins	Pathogen	Identity
1	Transcriptional regulator *PtxR* (Pyoverdine)	*Pseudomonas aeruginosa* PAO1	30 %
2	DNA-binding transcriptional activator AllS (allS)	*Klebsiella pneumoniae* subsp. pneumoniae NTUH-K2044	27 %
3	Transcriptional regulator (Pyoverdine)	*Pseudomonas aeruginosa* PAO1	26 %
4	*LysR* family transcriptional regulator (ACICU_RS04565)	*Acinetobacter baumanni* ACICU	25 %

biosynthesis occurs in both plants and bacteria through a non-13-hydroxylation pathway, indicating a parallel pathway between both plants and bacteria[54]. These results indicate a strong correlation between gibberellin production, growth promotion, and increased crop yield in plants.[55].

Cytokinins (CKs) play a significant role in plant shoot development. These isoprenoid-substituted adenine molecules exist in various forms, such as *cis*-zeatin, dihydrozeatin, *trans*-zeatin, and N6- (Δ2-isopentenyl)-adenine (iP), and are synthesised by isopentyltransferases (Taylor et al., 2003). The key genes involved in direct cytokinin biosynthesis include *LOG* (LONELY GUY), *AHK2_3_4 CKX, IPT, miaA, NDPS1*, and *miaB*. The finding of the present study is supported by the existence of the cytokinin-producing enzyme, "Lonely guy" (LOG), encoded by the *Cg2612* gene in the bacterium *Corynebacterium glutamicum,* as well as the presence of the *IPT* (isopently transferases) gene, a crucial regulator of cytokinin homeostasis and plant growth, which further strengthens this assertion.[56] Many studies have documented that several strains have the capacity for cytokinin production. These strains include *Bacillus subtilis*, *Paenibacillus polymyxa, P. fluorescens*, and *Rhizobium* sp..[22].

The gene clusters associated with biological nitrogen fixation were identified within the PM1 genome along with key regulatory genes involved in nitrogen metabolism (Table 5' Fig. S5). These findings were reconfirmed by the growth of PM1 in nitrogen-free media. The similar genes involved in nitrogen assimilation have been identified in *Azotobacter chroococcum* 76A, enabling tomato plants to adapt to salt stress under low nitrogen conditions.[57] The nitrogen uptake was also found to be increased by treatment with *Ochrobactrum* sp. Pv2Z2 in common bean plants compared to the non-inoculated control plants.[37] Additionally, researchers have identified a novel nitrogen-fixing *Ochrobactrum* strain from the root nodules of *Acacia mangium*.[58].

The availability of phosphorus which is often constrained by its immobilized form in the soil, is a critical factor for plant growth. Endophytic bacteria contribute to phosphorus availability by synthesising phosphates and organic acids.[59] The PM1 bacterial genome reveals genes involved in the phosphate transport system, including *pstS, pstC, pstA, pstB*, and *phoB*. The *Pst* phosphate transport system, regulated by these genes, plays a role in enhanced phosphate uptake and internalisation of inorganic phosphate.[60] Our findings support previous studies that identified the same phosphate solubilisation genes (*pstABCS*) in *Pseudomonas aeruginosa*,[61] *B. cereus* strain 905,[47] and the metagenome of the host plant *Emilia sonchifolia*.[62].

The presence of multiple genes involved in iron transport and siderophore production in strain PM1 suggests its potential in enhancing iron bioavailability to plants. The genome analysis revealed the presence of genes such as *feoB, feoC, efeU, FTR, FTH1, and ABC.MN.P SMFs*, are involved in iron transport and play a significant role in siderophore synthesis. Similar genes associated with iron-siderophore transport and siderophore uptake have been reported in *Saccharibacillus brassicae* ATSA2T *Pseudomonas strains* B18 and CS51.[61,63,64].

Root colonisation is a crucial step in establishing the primary association between bacteria and plants. The secretion of plant exudates plays a significant role in attracting bacteria and establishing them in the plant endosphere as endophytes.[65] In the PM1 genome, a complete set of genes involved in flagellar biosynthesis (*fhEFG, fhLMNOPQR, flhAB, flgABCDE, flgGHIJK, fliC*), chemotaxis (*motA, motB, fliGMN*), and biofilm formation (*hfq, crp, rpo*), which are associated with root colonization. The data corroborates with other reports in which similar genes were identified that were associated with root colonisation.[47].

Further, gene clusters with potential roles in combating abiotic stresses were also annotated. These include genes encoding cold-active chaperones, heat shock proteins, oxidative stress proteins, and heavy metal stress proteins. Similar findings have been reported in *Bacillus* strain STB1 and *B. haematophila,* which showed genes related to cold and heat shock response and resistance against Fusarium wilt disease, respectively.[47,66].

While our study focused on PGPR traits, it is important to note that whether strain PM1 possesses any genes associated with virulence is based on the PIFR and VFDB databases. However, the absence of secreted effector proteins and a limited complement of assembly proteins suggest a narrow pathogenic potential. Nonetheless, further experimental evidence is required to fully elucidate the true pathogenic potential of *B. anthropi* PM1. Similar findings have been reported in studies on *Leclercia* and *Yersinia* species, which identified 126–140 putative virulence-related proteins but concluded that the pathogenic capacity of these strains was limited.[45] Additionally, a study involving comparative genomic analyses of the *Brucella* genus showed no similarity between PM1 and virulence-related genes reported in *Brucella* strains.[45,67] These findings further support the opinion that the

Table 8
Secondary metabolite gene clusters identified using antiSMASH analysis.

Region	Genome region		Known Cluster				
	From	To	Type	Productions	Functions	Similarity	References
1.1	66,486	127,232	Acyl amino acids	Amabactin	–	25 %	Schimming et al., 2014
2.1	64,233	85,066	Terpene	–		–	–
2.2	90,986	132,167	Arylpolyene	TVA-YJ-2	Anti-tumor activity	4 %	Hu et al., 2022
3.1	99,754	120,655	NAGGN	oryzanaphthopyran A oryzanaphthopyran B oryzanaphthopyran C oryzanthrone A oryzanthrone B chlororyzanthrone A chlororyzanthrone B	Polyketides (GlsB/YeaQ/YmgE family stress response membrane protein)	6 %	Deng et al., 2024
4.1	62,798	90,609	Betalactone	Corynecin III/ Corynecin II/ Corynecin I	broad antibacterial spectrum (like- chloramphenico) Liu et al., 2022	13 %	Undabarrena et al., 2021
5.1	38,511	48,897	Ectoine	–	–	–	–
5.2	110,552	123,384	Hydrogen-cyanide	–	–	–	–
12.1	125,093	157,787	NI-siderophore	Orchrobactin	Siderophore (Biocontrol activity in plant) Lee et al., 2020	85 %	*Ochrobactrum anthropi* [7]
13.1	106,245	126,868	Hserlactone	–	–	–	–

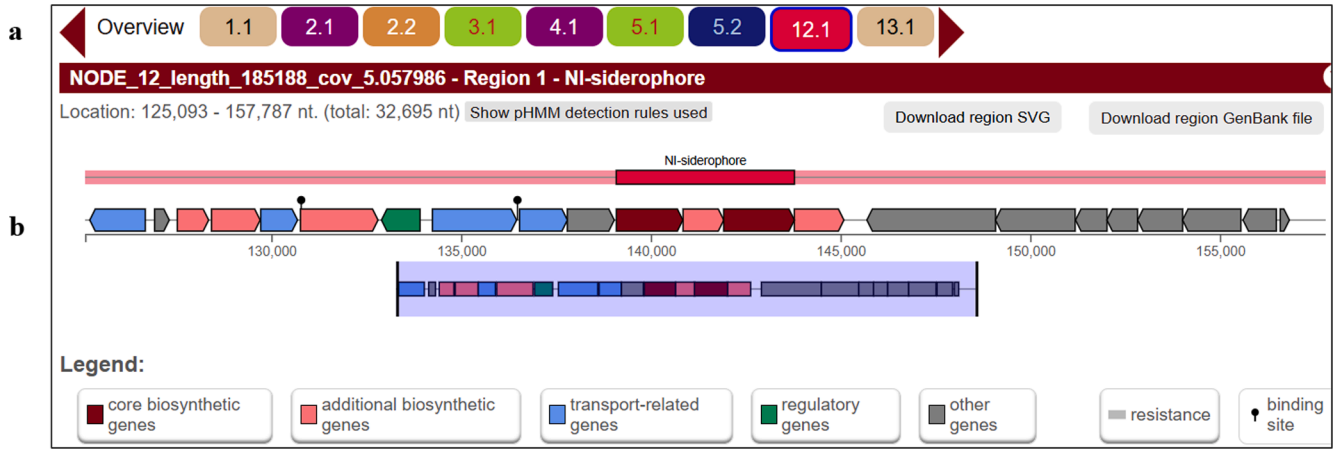

Fig. 7. Secondary metabolite gene cluster prediction based on antiSMASH analysis: total regions of gene cluster (a) and potential siderophore region (b).

pathogenic potential of *B. anthropi* PM1 could be minimal. Furthermore, prior studies have emphasised the safety of using *Brucella* species as plant growth-promoting bacteria.[37,46,68–70].

Plant-associated microbes benefit plants through various direct and indirect effects. The *Brucella* PM1 possesses genes associated with the biosynthesis of the ochrobactin siderophore, which has stress alleviation and growth promotion abilities.[71] The present findings align with the presence of the ochrobactin siderophore in the *Brucella* T16R-87 genome, which aids in iron acquisition and subsequently reduces phytopathogen attacks, making it a potential biocontrol agent.[19,72] Additionally, identified gene clusters such as oryzanaphthopyran (polyketides)[73] and Corynecin,[74] along with unidentified clusters such as terpenes, Hserlactone, and ectoine, may play a role in the disease-suppressive functions of plant-associated microbes.[75].

5. Conclusions

The present study provides insights into *B. anthropi* as an endophyte found in the pomegranate, *Lythraceae* family. Through 16S rDNA identification and whole genome sequencing, the genetic identity of the isolated endophyte was confirmed as *B. anthropi* ATCC 49188, with a genome length of 5,200,895 bp. The primary aim of this research was to investigate the plant growth-promoting traits (PGPTs) associated with *Brucella* endophytes in pomegranates, aiming to establish a genetic basis for their growth-promoting abilities. The analysis of *Brucella* genes revealed their involvement in crucial biological pathways, including nitrogen metabolism, hormone biosynthesis, phosphate solubilisation, and siderophore formation. Notably, the presence of the siderophore orchrobactin was observed through secondary metabolite analyses. These findings shed light on the potential biological functions of these genes. The present study contributes to understanding and enriching the knowledge of the genetic mechanisms underlying the growth-promoting traits of *Brucella anthropi* in pomegranates, offering further research and applications in sustainable agriculture.

CRediT authorship contribution statement

Poonam Patel: Writing – original draft, Validation, Methodology, Investigation, Formal analysis. **Fenil Patel:** Supervision, Investigation, Formal analysis, Data curation. **Chaitanya Joshi:** Visualization, Supervision, Resources, Investigation, Funding acquisition. **Madhvi Joshi:** Visualization, Supervision, Project administration, Methodology, Funding acquisition.

Funding

The funding support was provided by the Department for Science and Technology, Government of Gujarat.

Declaration of competing interest

The authors declare that they have no known competing financial interests or personal relationships that could have appeared to influence the work reported in this paper.

Appendix A. Supplementary material

Supplementary data to this article can be found online at https://doi.org/10.1016/j.jgeb.2025.100486.

Data availability

Data will be made available on request.

The data analyzed during the present investigation are available from the corresponding author upon reasonable request.

References

1. Kandel SL, Joubert PM, Doty SL. Bacterial endophyte colonization and distribution within plants. *Microorganisms*. 2017;5:77.
2. Singh R, Pandey KD, Singh M, et al. Isolation and characterization of endophytes bacterial strains of Momordica charantia L. and their possible approach in stress management. *Microorganisms*. 2022;10:290.
3. Zeynalova AM, Origin NEN. taxonomy and systematics of pomegranate. *Proc Inst Bot Azerbaijan Natl Acad Sci*. 2017;37.
4. Desai P, Patil G, Dholiya B, Desai S, Patel F, Narayanan S. Development of an efficient micropropagation protocol through axillary shoot proliferation for pomegranate variety 'Bhagwa.'. *Ann Agrar Sci*. 2018;16:444–450.
5. Karn M, Sharma SK, Sharma A, Pal J. Isolation and characterization of endophytes against bacterial blight of pomegranate. *Int J Bio-Resource Stress Manag*. 2022;13:683–692.
6. Bacon C, Hinton D. Bacterial endophytes: the endophytic niche, its occupants, and its utility. *Plant-Associated Bact*. 2006:155–194.
7. Kanani P, Modi A, Kumar A. *Biotization of endophytes in micropropagation: A helpful enemy*. Microb. Endophytes: Elsevier; 2020:357–379.
8. Afzal I, Shinwari ZK, Sikandar S, Shahzad S. Plant beneficial endophytic bacteria: Mechanisms, diversity, host range and genetic determinants. *Microbiol Res*. 2019;221:36–49.
9. Conn VM, Franco CMM. Analysis of the endophytic actinobacterial population in the roots of wheat (Triticum aestivum L.) by terminal restriction fragment length polymorphism and sequencing of 16S rRNA clones. *Appl Environ Microbiol*. 2004;70:1787–1794.
10. Husen E. Screening of soil bacteria for plant growth promotion activities in vitro. *Indones J Agric Sci*. 2003;4:27–31.
11. Lebeis SL. The potential for give and take in plant–microbiome relationships. *Front Plant Sci*. 2014;5:97418.
12. Halo BA, Khan AL, Waqas M, et al. Endophytic bacteria (Sphingomonas sp. LK11) and gibberellin can improve Solanum lycopersicum growth and oxidative stress under salinity. *J Plant Interact*. 2015;10:117–125.
13. Deng Z-S, Zhang B-C, Qi X-Y, et al. Root-associated endophytic bacterial community composition of Pennisetum sinese from four representative provinces in China. *Microorganisms*. 2019;7:47.
14. Roodi D, Millner JP, McGill C, Johnson RD, Jauregui R, Card SD. Methylobacterium, a major component of the culturable bacterial endophyte community of wild Brassica seed. *PeerJ*. 2020;8:e9514.
15. Ma Y, Tan X, Liu J, Luo W, Huang S. Identification of an endophytic biocontrol strain NS03 and its efficacy in controlling pomegranate dry fruit rot disease. *Acta Hortic*. 2015:145–151.
16. Shahaby AF, Alharthi AA, El Tarras AE. Screening of natural bacterial flora of pomegranate roots (Punica granatum L.) and their antibiotic activity in Taif, Saudi Arabia. *Int J Curr Microbiol App Sci*. 2016;5:1–6.
17. Kaul S, Sharma TK, Dhar M. "Omics" tools for better understanding the plant–endophyte interactions. *Front Plant Sci*. 2016;7:955.
18. Satam H, Joshi K, Mangrolia U, et al. Next-generation sequencing technology: current trends and advancements. *Biology (basel)*. 2023;12:997.
19. Lee SA, Sang MK, Song J, Kwon S-W, Weon H-Y. Complete genome sequence of Brucella anthropi strain T16R-87 isolated from tomato (Solanum lycopersicum L.) rhizosphere. *Microbiol Soc Korea*. 2020;56:430–432.
20. Jasim B, Joseph AA, John CJ, Mathew J, Radhakrishnan EK. Isolation and characterization of plant growth promoting endophytic bacteria from the rhizome of Zingiber officinale. *3 Biotech*. 2014;4:197–204.
21. Collins MD, Falsen E, Brownlee K, Lawson PA. Helcococcus sueciensis sp. nov., isolated from a human wound. *Int J Syst Evol Microbiol*. 2004;54:1557–1560.
22. dos Santos RM, Diaz PAE, Lobo LLB, Rigobelo EC. Use of plant growth-promoting rhizobacteria in maize and sugarcane: characteristics and applications. *Front Sustain Food Syst*. 2020;4:136.
23. Marakana T, Sharma M, Sangani K. Isolation and characterization of halotolerant bacteria and it's effects on wheat plant as PGPR. *Pharma Innov J*. 2018;7:102–110.
24. Madhaiyan M, Alex THH, Te NS, Prithiviraj B, Ji L. Leaf-residing Methylobacterium species fix nitrogen and promote biomass and seed production in Jatropha curcas. *Biotechnol Biofuels*. 2015;8:1–14.
25. Himpsl SD, Mobley HLT. Siderophore detection using chrome azurol S and cross-feeding assays. *Proteus Mirabilis Methods Protoc*. 2019:97–108.
26. Andrews S. FastQC: a quality control tool for high throughput sequence data. 2010 2017.
27. Bankevich A, Nurk S, Antipov D, et al. SPAdes: a new genome assembly algorithm and its applications to single-cell sequencing. *J Comput Biol*. 2012;19:455–477.
28. Meier-Kolthoff JP, Göker M. TYGS is an automated high-throughput platform for state-of-the-art genome-based taxonomy. *Nat Commun*. 2019;10:2182.
29. Tanizawa Y, Fujisawa T, Nakamura Y. DFAST: a flexible prokaryotic genome annotation pipeline for faster genome publication. *Bioinformatics*. 2018;34:1037–1039.
30. Wattam AR, Davis JJ, Assaf R, et al. Improvements to PATRIC, the all-bacterial bioinformatics database and analysis resource center. *Nucleic Acids Res*. 2017;45:D535–D542.
31. Cantalapiedra CP, Hernández-Plaza A, Letunic I, Bork P, Huerta-Cepas J. eggNOG-mapper v2: functional annotation, orthology assignments, and domain prediction at the metagenomic scale. *Mol Biol Evol*. 2021;38:5825–5829.
32. Patz S, Gautam A, Becker M, Ruppel S, Rodríguez-Palenzuela P, Huson DH. PLaBAse: A comprehensive web resource for analyzing the plant growth-promoting potential of plant-associated bacteria. *Biorxiv*. 2021:2012–2021.
33. Aramaki T, Blanc-Mathieu R, Endo H, et al. KofamKOALA: KEGG Ortholog assignment based on profile HMM and adaptive score threshold. *Bioinformatics*. 2020;36:2251–2252.
34. Chen L, Yang J, Yu J, et al. VFDB: a reference database for bacterial virulence factors. *Nucleic Acids Res*. 2005;33:D325–D328.
35. Blin K, Shaw S, Kloosterman AM, et al. antiSMASH 6.0: improving cluster detection and comparison capabilities. *Nucleic Acids Res*. 2021;49:W29–W35.
36. Trujillo ME, Willems A, Abril A, et al. Nodulation of Lupinus albus by strains of Ochrobactrum lupini sp. nov. *Appl Environ Microbiol*. 2005;71:1318–1327.
37. Imran A, Saadalla MJA, Khan S-U, Mirza MS, Malik KA, Hafeez FY. Ochrobactrum sp. Pv2Z2 exhibits multiple traits of plant growth promotion, biodegradation and N-acyl-homoserine-lactone quorum sensing. Ann Microbiol 2014;64:1797–806.
38. Zurdo-Pineiro JL, Rivas R, Trujillo ME, et al. Ochrobactrum cytisi sp. nov., isolated from nodules of Cytisus scoparius in Spain. *Int J Syst Evol Microbiol*. 2007;57:784–788.
39. Lebuhn M, Achouak W, Schloter M, et al. Taxonomic characterization of Ochrobactrum sp. isolates from soil samples and wheat roots, and description of Ochrobactrum tritici sp. nov. and Ochrobactrum grignonense sp. nov. *Int J Syst Evol Microbiol*. 2000;50:2207–2223.
40. Jain C, Rodriguez-R LM, Phillippy AM, Konstantinidis KT, Aluru S. High throughput ANI analysis of 90K prokaryotic genomes reveals clear species boundaries. *Nat Commun*. 2018;9:5114.
41. Vandenkoornhuyse P, Quaiser A, Duhamel M, Le Van A, Dufresne A. The importance of the microbiome of the plant holobiont. *New Phytol*. 2015;206:1196–1206.
42. Wang Y, Zhao Q, Sun Z, et al. Whole-genome analysis revealed the growth-promoting mechanism of endophytic bacterial strain Q2H1 in potato plants. *Front Microbiol*. 2022;13, 1035901.
43. Rossi-Tamisier M, Benamar S, Raoult D, Fournier P-E. Cautionary tale of using 16S rRNA gene sequence similarity values in identification of human-associated bacterial species. *Int J Syst Evol Microbiol*. 2015;65:1929–1934.
44. Yang L-L, Zhi X-Y, Li W-J. Phylogenetic analysis of Nocardiopsis species based on 16S rRNA, gyrB, sod and rpoB gene sequences. *Wei Sheng Wu Xue Bao= Acta Microbiol Sin*. 2007;47:951–955.
45. Maddock D, Arnold D, Denman S, Brady C. Description of a novel species of Leclercia, Leclercia tamurae sp. nov. and proposal of a novel genus Silvania gen. nov. containing two novel species Silvania hatchlandensis sp. nov. and Silvania confinis sp. nov. isolated from the rhizosphere of oak. *BMC Microbiol*. 2022;22:289.
46. Meng X, Yan D, Long X, Wang C, Liu Z, Rengel Z. Colonization by endophytic O chrobactrum anthropi M n1 promotes growth of J erusalem artichoke. *Microb Biotechnol*. 2014;7:601–610.
47. Adeleke BS, Ayangbenro AS, Babalola OO. Genomic analysis of endophytic Bacillus cereus T4S and its plant growth-promoting traits. *Plants*. 2021;10:1776.
48. Palberg D, Kisiała A, Jorge GL, Emery RJN. A survey of Methylobacterium species and strains reveals widespread production and varying profiles of cytokinin phytohormones. *BMC Microbiol*. 2022;22:49.
49. Wang Y, Sun Z, Zhao Q, et al. Whole-genome analysis revealed the growth-promoting and biological control mechanism of the endophytic bacterial strain Bacillus halotolerans Q2H2, with strong antagonistic activity in potato plants. *Front Microbiol*. 2024;14, 1287921.
50. Asaf S, Khan AL, Khan MA, Al-Harrasi A, Lee I-J. Complete genome sequencing and analysis of endophytic Sphingomonas sp. LK11 and its potential in plant growth. *3 Biotech*. 2018;8:1–14.
51. Coulson TJD, Patten CL. Complete genome sequence of Enterobacter cloacae UW5, a rhizobacterium capable of high levels of indole-3-acetic acid production. *Genome Announc*. 2015;3:10–1128.
52. Gray WM. Hormonal regulation of plant growth and development. *PLoS Biol*. 2004;2:e311.

53. Tully R, van Berkum P, Lovins K, Keister D. Identification and sequencing of a cytochrome P450 gene cluster from Bradyrhizobium japonicum. *Biochim Biophys Acta (BBA)-Gene Struct Expr*. 1998;1398:243–255.
54. Salazar-Cerezo S, Martínez-Montiel N, García-Sánchez J, Pérez-y-Terrón R, Martínez-Contreras RD. Gibberellin biosynthesis and metabolism: A convergent route for plants, fungi and bacteria. *Microbiol Res*. 2018;208:85–98.
55. Bottini R, Cassán F, Piccoli P. Gibberellin production by bacteria and its involvement in plant growth promotion and yield increase. *Appl Microbiol Biotechnol*. 2004;65:497–503.
56. Akhtar SS, Mekureyaw MF, Pandey C, Roitsch T. Role of cytokinins for interactions of plants with microbial pathogens and pest insects. *Front Plant Sci*. 2020;10, 470181.
57. Van Oosten MJ, Di Stasio E, Cirillo V, et al. Root inoculation with Azotobacter chroococcum 76A enhances tomato plants adaptation to salt stress under low N conditions. *BMC Plant Biol*. 2018;18:1–12.
58. Ngom A, Nakagawa Y, Sawada H, et al. A novel symbiotic nitrogen-fixing member of the Ochrobactrum clade isolated from root nodules of Acacia mangium. *J Gen Appl Microbiol*. 2004;50:17–27.
59. Varga T, Hixson KK, Ahkami AH, et al. Endophyte-promoted phosphorus solubilization in Populus. *Front Plant Sci*. 2020;11, 567918.
60. Hudek L, Premachandra D, Webster WAJ, Bräu L. Role of phosphate transport system component PstB1 in phosphate internalization by Nostoc punctiforme. *Appl Environ Microbiol*. 2016;82:6344–6356.
61. Singh P, Singh RK, Guo D-J, et al. Whole genome analysis of sugarcane root-associated endophyte Pseudomonas aeruginosa B18—A plant growth-promoting bacterium with antagonistic potential against Sporisorium scitamineum. *Front Microbiol*. 2021;12, 628376.
62. Urumbil SK, Anilkumar M. Metagenomic insights into plant growth promoting genes inherent in bacterial endophytes of Emilia sonchifolia (Linn.) DC. *Plant Sci Today*. 2021;8:6–16.
63. Jiang L, Seo J, Peng Y, et al. Genome insights into the plant growth-promoting bacterium Saccharibacillus brassicae ATSA2T. *AMB Express*. 2023;13:9.
64. Kang S-M, Asaf S, Khan AL, Lubna KA, Mun B-G, et al. Complete genome sequence of Pseudomonas psychrotolerans CS51, a plant growth-promoting bacterium, under heavy metal stress conditions. *Microorganisms*. 2020;8:382.
65. Ellouze W, Hamel C, Bouzid S, St-Arnaud M. Root endophytes modify the negative effects of chickpea on the emergence of durum wheat. *Appl Soil Ecol*. 2015;96:201–210.
66. Khanna A, Raj K, Kumar P, Wati L. Antagonistic and growth-promoting potential of multifarious bacterial endophytes against Fusarium wilt of chickpea. *Egypt J Biol Pest Control*. 2022;32:17.
67. Papaparaskevas J, Procopiou A, Routsias J, Vrioni G, Tsakris A. Detection of virulence-associated genes among brucella melitensis and brucella abortus clinical isolates in Greece, 2001–2022. *Pathogens*. 2023;12:1274.
68. Faisal M, Hasnain S. Growth stimulatory effect of Ochrobactrum intermedium and Bacillus cereus on Vigna radiata plants. *Lett Appl Microbiol*. 2006;43:461–466.
69. Chakraborty U, Chakraborty BN, Basnet M, Chakraborty AP. Evaluation of Ochrobactrum anthropi TRS-2 and its talc based formulation for enhancement of growth of tea plants and management of brown root rot disease. *J Appl Microbiol*. 2009;107:625–634.
70. Riaz S, Faisal M, Hasnain S. Cicer arietinum growth promotion by Ochrobactrum intermedium and Bacillus cereus in the presence of CrCl 3 and K 2 CrO 4. *Ann Microbiol*. 2010;60:729–733.
71. Singh P, Chauhan PK, Upadhyay SK, et al. Mechanistic insights and potential use of siderophores producing microbes in rhizosphere for mitigation of stress in plants grown in degraded land. *Front Microbiol*. 2022;13, 898979.
72. Ahmed E, Holmström SJM. Siderophores in environmental research: roles and applications. *Microb Biotechnol*. 2014;7:196–208.
73. Deng Y, Li C-J, Zhang J, Yu W-H, Liu L-Y, Zhang Y-Q. Extensive genomic study characterizing three Paracoccaceae populations and revealing Pseudogemmobacter lacusdianii sp. nov. and Paracoccus broussonetiae sp. nov. *Microbiol Spectr*. 2024;12, e01088.
74. Liu S-W, Jadambaa N, Nikandrova AA, Osterman IA, Sun C-H. Exploring the diversity and antibacterial potentiality of cultivable actinobacteria from the soil of the saxaul forest in southern Gobi desert in Mongolia. *Microorganisms*. 2022;10:989.
75. Carrión VJ, Perez-Jaramillo J, Cordovez V, et al. Pathogen-induced activation of disease-suppressive functions in the endophytic root microbiome. *Science (80-)*. 2019;366:606–612.